SUPPORTING INFORMATION

Early Detection of Biofouling on Water Purification Membranes by Ambient Ionization Mass Spectrometry Imaging

Swathy Jakka Ravindran[1], *Ramesh Kumar*[1], *Amitava Srimany*[1], *Ligy Philip*[2] *and Thalappil Pradeep*[1*]

[1]DST Unit of Nanoscience (DST UNS) and Thematic Unit of Excellence (TUE), Department of Chemistry, Indian Institute of Technology Madras, Chennai 600 036, India.

[2]EWRE Division, Department of Civil Engineering, Indian Institute of Technology Madras, Chennai 600036, India.

*Corresponding Author: (T.P.) E-mail: pradeep@iitm.ac.in. Fax: +91-44-2257-0545.

CONTENT:

SUPPORTING INFORMATION 1:

Growth of Biofilm - Experimental

Static biofilms: Cell suspensions in the petri dishes were diluted to 50x with the culture medium under sterile conditions. Pre-sterilized water purification membranes and other substrates of interest were fully submerged in the nutrient mixture. Static biofilms were permitted to grow for 72 h at 30 °C. Growth medium was then removed from the petri dishes by pipette and the biofilms were allowed to air-dry completely prior to the preparation for mass spectral analysis[35].

Biofilms in continuous flow: P. aeruginosa was grown to a final optical density (600 nm) of 1 and the cells were suspended in the RO unit for the growth of the biofilm. An enriched synthetic wastewater medium was used for bacterial growth in the RO crossflow test unit. The chemical composition chosen for the synthetic wastewater is a modified protocol of Moshe Herzberg and Menachem Elimelech[26], based on natural water quality with moderate biological processes. To achieve an enhanced biofouling behavior, relatively high concentrations of nutrients and carbon energy sources were designed. Specifically, to prepare the synthetic feed water, deionized water (DI) was supplemented with 250 ppm of NaCl and 0.25 mM Glucose. In addition, 1 ml of LB broth was added per 1 l of the solution[1, 35]. The final pH was 7.4.

SUPPORTING INFORMATION 2:

Extraction of Biofilms from substrates

The biofilm extract was prepared by collecting submerged 2x2 cm^2 coverslips, after rinsing twice with sterile distilled water. About 1 mL of extraction solution (50/50 (v/v%) MeOH:H_2O + 0.1% AcOH) was added to each coverslip and was shaken vigorously for 15 min. This extract was centrifuged for 5 min at 3000 g. The supernatant was diluted 100 times before injection.

SUPPORTING INFORMATION 3:

Crossflow test unit – Experimental setup

A commercial thin film composite, 'ULP18112-75 domestic tap water RO membrane' (Vontron, China) was used as a model membrane for all the biofouling experiments. The laboratory-scale test unit consisted of one flat sheet membrane cell with a membrane coupon of active surface area and feed spacer thickness of 24.1 cm^2 and 0.7 mm, respectively, operating in re-circulation mode. The feed tank was filled with 3 L of synthetic feed water spiked with 10^5 CFU/mL of *P. aeruginosa* and was replaced every 5 hours to avoid the feed tank to act as a bioreactor. The operating pressure was kept constant at 40 psi with a cross flow velocity of 0.65 meter/sec. Both

permeate and retentate were recirculated back to the feed reservoir. Five sets of individual experiments were conducted at 1, 2, 3, 4 and 5 days of operation. During each set, feed was stopped for 12 hours alternatively allowing the growth of biofilm. The lab scale unit was carefully cleaned each time before running fresh membrane coupons. Prior to experiments with synthetic feed water, membrane coupons were compacted by operating with autoclaved (DI) water to 60 psi for 5 hours. Biofilm grown samples (digital image shown in Figure 2a) were collected as such, stored and analyzed using DESI MS to track the molecular signals of different stages of biofilm.

SUPPORTING FIGURE S1:

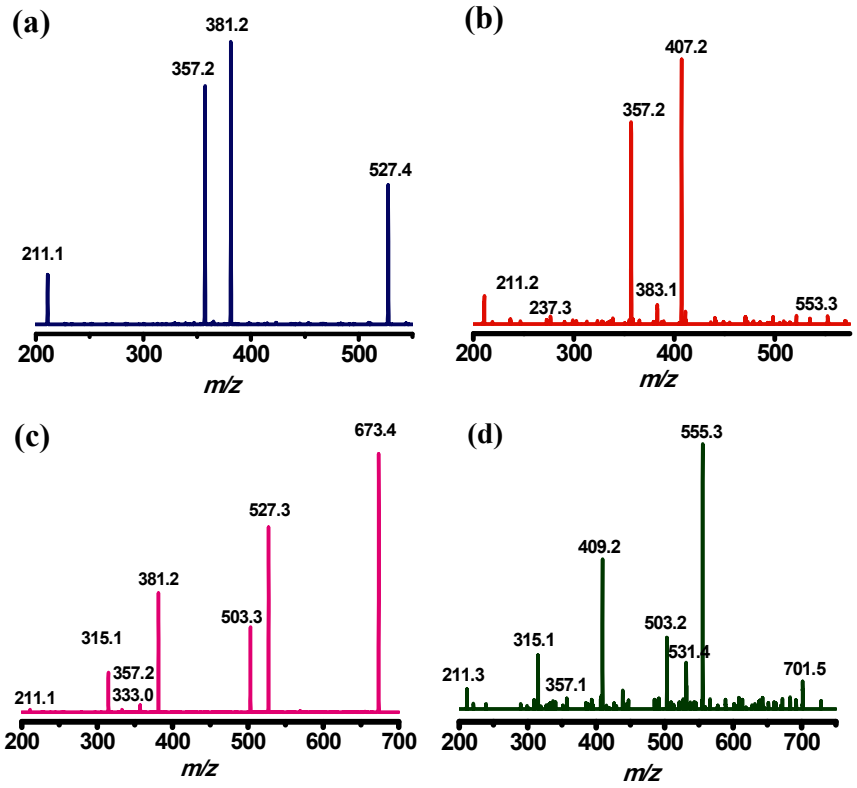

Figure S1: MS/MS product ion spectra of the sodium adduct of rhamnolipid standards. Fragmentation pattern of commercial standards of mono and di-rhamnolipids. (a) *m/z* 527.3, (b) 553.4 (c) 673.4 (d) 701.4.

SUPPORTING FIGURE S2:

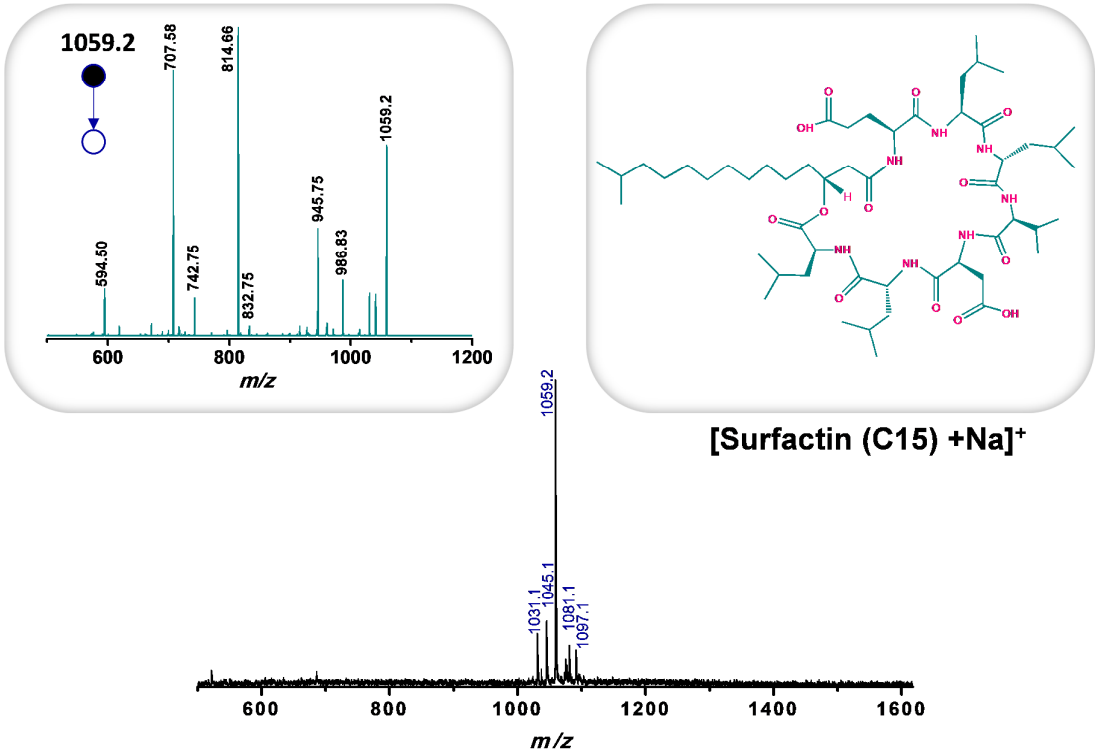

Figure S2: Positive mode DESI mass spectrum of gram positive bacterial biofilm recorded from nylon membranes and corresponding MS/MS product ion spectrum. Mass spectrum of *Bacillus subtilis* (ATCC 21331) biofilm observed in positive ion mode showing *m/z* 1059.2. The specified peak represents the sodium adduct of surfactin (C15) secreted by *B. subtilis* at initial stages (24 h) of adsorption on the surfaces. Fragmentation pattern of surfactin secreted by the organism during the biofilm growth and its deduced structure are shown in the insets.

SUPPORTING FIGURE S3:

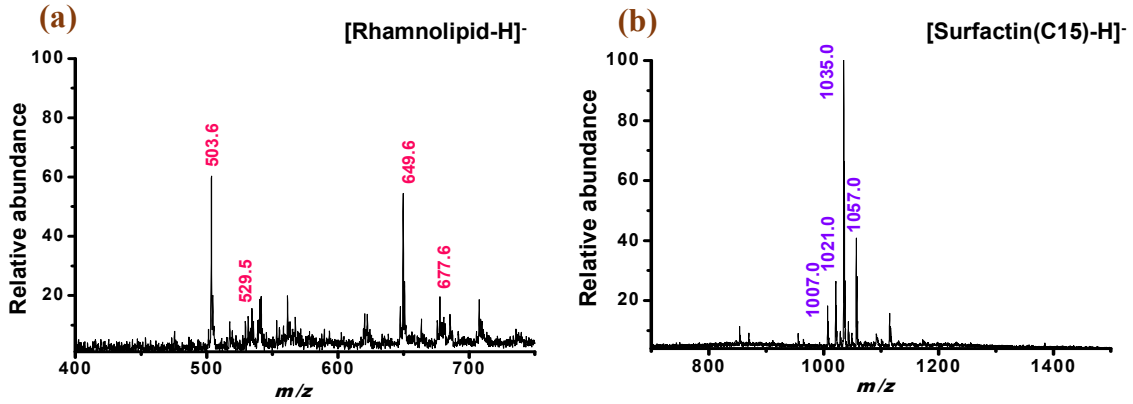

Figure S3: Negative mode DESI mass spectra of biofilms recorded from nylon membranes. (a) Mass spectrum of *Pseudomonas aeruginosa* (ATCC 25619) biofilm observed in negative mode. (b) Mass spectrum of *Bacillus subtilis* (ATCC 21331) biofilm observed in negative mode. The specified peaks represent the rhamnolipids and surfactin secreted by *P. aeruginosa* and *B. subtilis* at initial stages (24 h) of adsorption on the surfaces.

SUPPORTING FIGURE S4:

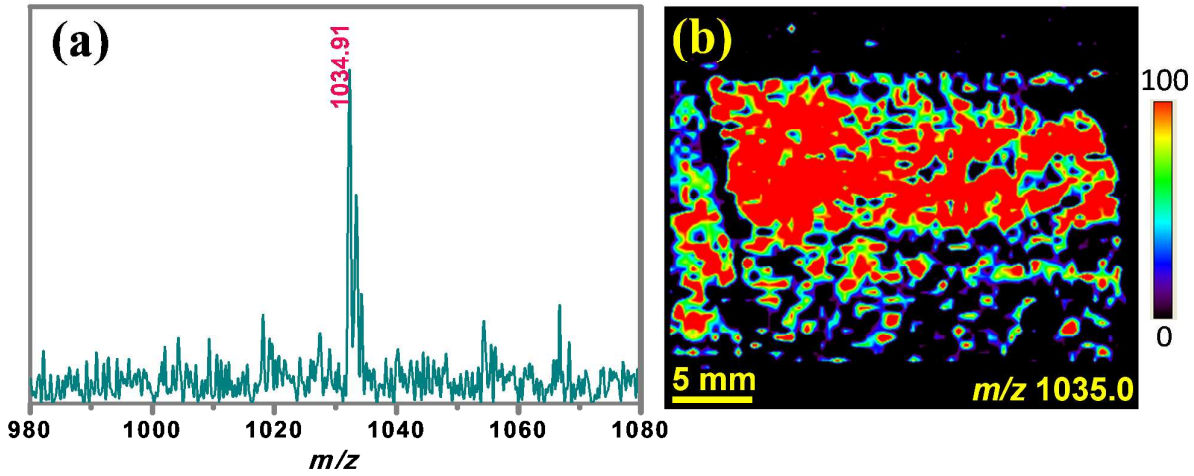

Figure S4: DESI MSI of a *B. subtilis* biofilm. (a) Negative ion DESI mass spectrum of *Bacillus subtilis* recorded directly on nylon membranes. (b) Single *m/z* mass spectrometric image of surfactin.

SUPPORTING FIGURE S5:

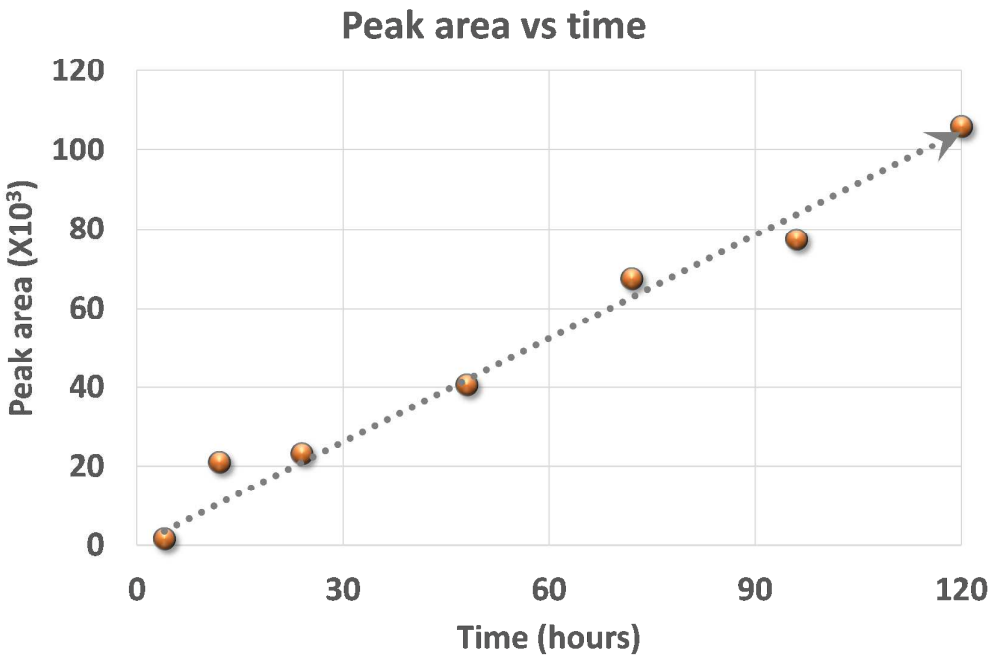

Figure S5: A peak area vs time plot of rhamnolipids secreted at different ages of the biofilm. The dynamic biofilm growth is demonstrated by studying the signal intensity of the signature analyte *m/z* 673.3 from the acquired mass spectra, exhibiting modest linearity with time.

SUPPORTING FIGURE S6:

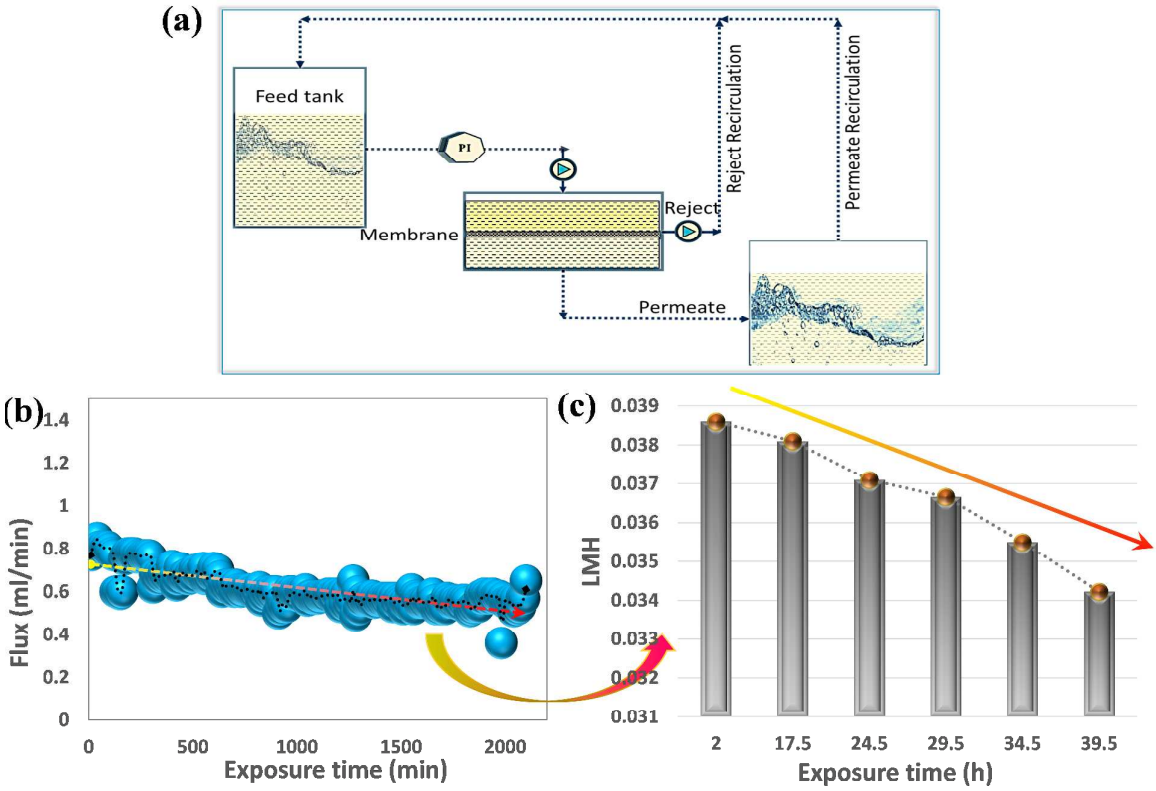

Figure S6: Biofouling study on RO membrane using cross flow test unit. (a) Schematic representation of the laboratory-scale RO membrane test unit. (b) Decrease in permeation due to biofilm development, plotted with time. (c) Small change in the flux thorough the used membrane coupon area, denoted by the increase in analyte molecule.

SUPPORTING FIGURE S7:

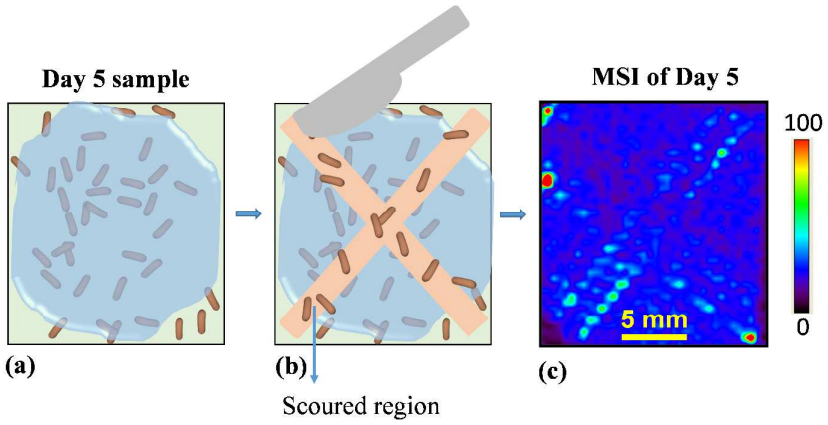

Figure S7: Revealing rhamnolipids beneath the EPS cover. (a) and (b) shows a schematic representation of a fully developed biofilm and the scouring off of the EPS layer in the indicated directions. (c) DESI MSI of the membrane showing increase in intensity of rhamnolipids in the regions exposed.

SUPPORTING FIGURE S8:

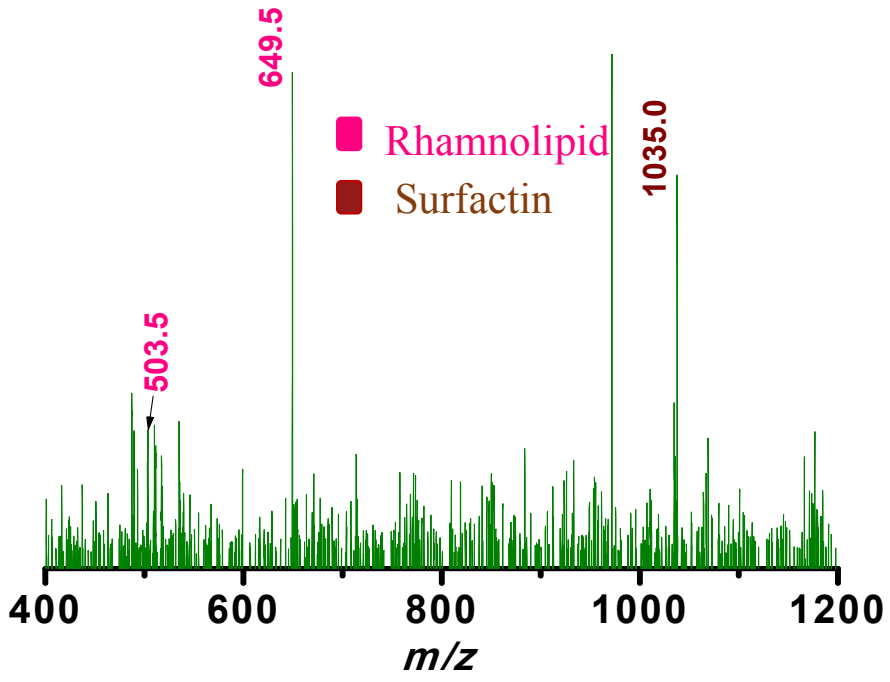

Figure S8. Positive mode DESI mass spectrum of species specific biofilm identification/differentiation. *Pseudomonas* and *Bacillus* biofilms expressed on the same membrane, show signals of both rhamnolipid and surfactin simultaneously.

SUPPORTING FIGURE S9:

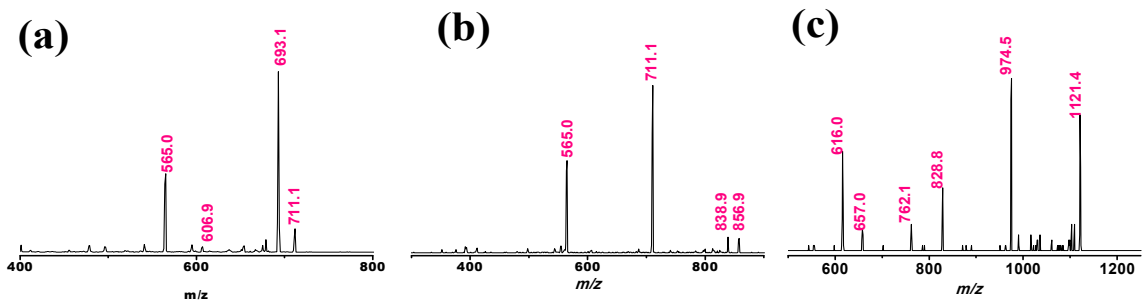

Figure S9. MS/MS product ion spectra of the Rhamnolipid-Metal complexes. Positive ion ESI-MS-MS spectra of Rhamnolipid – Pb^{2+} complex. (a) *m/z* 711.1, (b) *m/z* 856.9; Positive ion ESI-MS-MS spectrum of Rhamnolipid – Cd^{2+} complex. (c) *m/z* 1121.4; normalised collision energy (CE) at 30 to 50 (manufacturer's unit).

SUPPORTING TABLE S1:

Table S1: Positive ion mode mass spectrometric assignments for solutions containing Rhamnolipid/ Rhamnolipid + M^+ (Cd^{2+}/Pb^{2+}).

S.N	*m/z*	Category	Assignments
1	505.2	Mono-RL	$[(Rha\text{-}C10\text{-}C10)H]^+$
2	522.1	Mono-RL	$[(Rha\text{-}C10\text{-}C10)NH_4]^+$
3	527.4	Mono-RL	$[(Rha\text{-}C10\text{-}C10)Na]^+$
4	543.2	Mono-RL	$[(Rha\text{-}C8\text{-}C10)K]^+$
5	553.4	Mono-RL	$[(Rha\text{-}C10\text{-}C12:1)Na]^+$
6	555.4	Mono-RL	$[(Rha\text{-}C10\text{-}C12)Na]^+$
7	565.1	Tails + Pb^{2+}	$[(C10\text{-}C10\ tails)Pb]^+$
8	650.9	Di-RL	$[(Rha\text{-}Rha\text{-}C10\text{-}C10)H]^+$
9	667.9	Di-RL	$[(Rha\text{-}Rha\text{-}C10\text{-}C10)NH_4]^+$
10	673.3	Di-RL	$[(Rha\text{-}Rha\text{-}C10\text{-}C10)Na]^+$
11	683.1	Mono-RL + Pb^{2+}	$[(Rha\text{-}C8\text{-}C10 - H)Pb]^+$
12	689.3	Di-RL	$[(Rha\text{-}Rha\text{-}C10\text{-}C10)K]^+$
13	701.3	Di-RL	$[(Rha\text{-}Rha\text{-}C10\text{-}C12)Na]^+$
14	711.1	Mono-RL + Pb^{2+}	$[(Rha\text{-}C10\text{-}C10 - H)Pb]^+$
15	856.9	Di-RL	$[(Rha\text{-}Rha\text{-}C10\text{-}C10 - H)Pb]^+$
16	884.9	Di-RL	$[(Rha\text{-}Rha\text{-}C10\text{-}C12 - H)Pb]^+$
17	1030.9	$(Mono\text{-}RL)_2$	$[(Rha\text{-}C10\text{-}C10)_2Na]^+$
18	1047.3	$(Mono\text{-}RL)_2$	$[(Rha\text{-}C10\text{-}C10)_2K]^+$
19	1075.4	$(Mono\text{-}RL)_2$	$[(Rha\text{-}C10\text{-}C10)(Rha\text{-}C10\text{-}C12:1)K]^+$
20	1121.2	$(Mono\text{-}RL)_2 + Cd^{2+}$	$[(Rha\text{-}C10\text{-}C10)(Rha\text{-}C10\text{-}C10\text{-}H)Cd]^+$
21	1149.1	$(Mono\text{-}RL)_2 + Cd^{2+}$	$[(Rha\text{-}C10\text{-}C10)(Rha\text{-}C10\text{-}C12\text{-}H)Cd]^+$
22	1242.8	$(Di\text{-}RL)_2$ + Pb^{2+}	$[(Rha\text{-}C10\text{-}C10)(Rha\text{-}C10\text{-}C12 - H)Pb]$
23	1301.5	$(Di\text{-}RL)_2$	$[(\ Rha\text{-}Rha\text{-}C10\text{-}C10)_2H]^+$
24	1339.2	$(Di\text{-}RL)_2$	$[(Rha\text{-}Rha\text{-}C10\text{-}C10)_2K]^+$
25	1413.1	$(Di\text{-}RL)_2 + Cd^{2+}$	$[(Rha\text{-}Rha\text{-}C10\text{-}C10)_2Cd]^+$
26	1441.1	$(Di\text{-}RL)_2 + Cd^{2+}$	$[(Rha\text{-}Rha\text{-}C10\text{-}C10)(Rha\text{-}Rha\text{-}C10\text{-}C12)Cd]^+$
27	1506.9	$(Di\text{-}RL)_2$ + Pb^{2+}	$[(Rha\text{-}Rha\text{-}C10\text{-}C10)_2Pb]^+$
28	1624.5	$(Mono\text{-}RL)_3 + Cd^{2+}$	$[(Rha\text{-}C10\text{-}C10 - H)_2\ (Rha\text{-}C10\text{-}C10)Cd]^+$